Supplemental material

Sohn et al., https://doi.org/10.1083/jcb.201710095

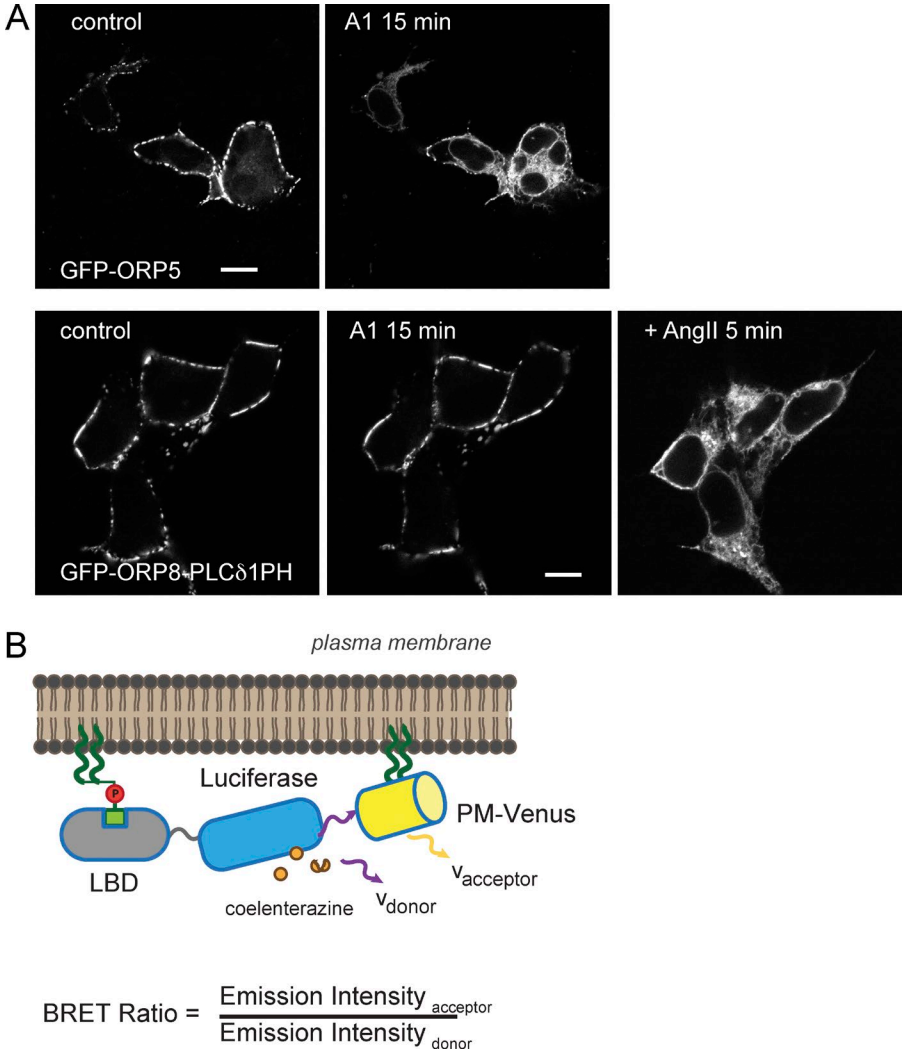

Figure S1. **PM engagement of ORP8-PLCδ-PH and principal of BRET analysis. (A)** Representative live-cell images comparing localization of ORP5 (top) or ORP8-PLCδ1-PH (bottom) in the presence of A1 (100 nM) or A1 plus AngII (100 nM). HEK293-AT1 cells were transfected with GFP-tagged ORP5 or ORP8-PLCδ1-PH and subjected to confocal microscopy after 1 d. Cells were observed with treatment of A1 or A1 plus AngII for the indicated time. Bars, 10 µm. **(B)** Schematic diagram describing the principal of BRET analysis. BRET signal is determined by measuring the proximity between lipid binding domain–fused *s*-luciferase and PM-anchored mVenus. In brief, PM-bound *s*-luciferase (donor) excites PM-anchored mVenus (acceptor) in the presence of coelenterazine h, which is a substrate of luciferase. A change in PM lipid levels increases or decreases PM binding of lipid binding domain–*s*-luciferase and, in turn, the excitation of mVenus. BRET ratio is defined by the emission intensity of mVenus (acceptor) per the emission intensity of *s*-luciferase (donor).

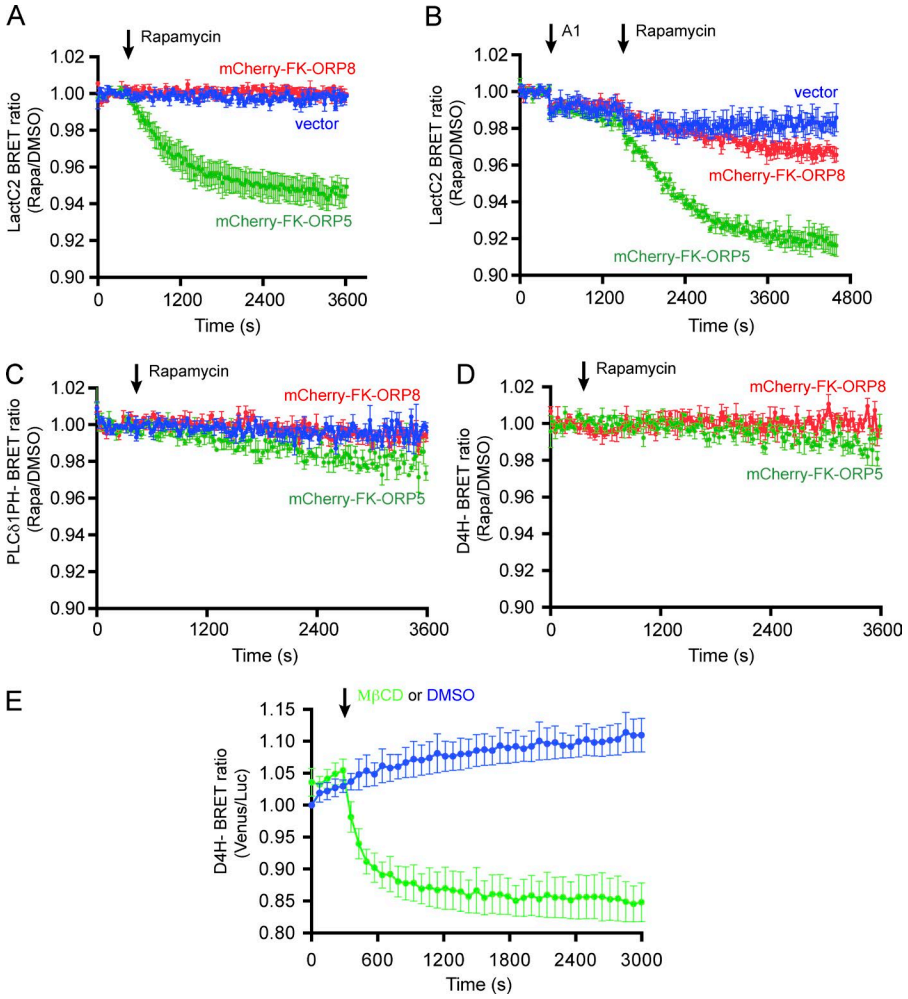

Figure S2. **Characterization of the abilities of recruitable ORP5/8 proteins to extract PS, PI(4,5)P_2, and cholesterol from the PM. (A)** Analysis of PS extraction from PM by PM-recruited ORP5/8. HEK293-AT1 cells were transfected with mCherry or mCherry-tagged FKBP-ORP5 (FK-ORP5) or -ORP8 (FK-ORP8) together with PM-targeted FRB (PM2-FRB). PM PS levels were quantitated with BRET analysis by measuring emission intensity of PM-anchored Venus acquired from Lact-C2–fused luciferase. After baseline measurement, cells were treated with DMSO or rapamycin (100 nM) to recruit FK-ORP5 or -ORP8 to the PM. PS level changes were plotted relative to DMSO-treated controls (rapamycin/DMSO). These ratio values were normalized to those obtained from pretreatment baseline measurement. Grand means ± SEM are shown from three independent experiments performed in triplicate. **(B)** Quantitation of PS extraction from PM by PM-recruited ORP5/8 after treatment with the PI4KA inhibitor, A1 (30 nM), for 10 min. PM PS quantitation was as described in A. Grand means ± SEM are shown from three independent experiments performed in triplicate. **(C)** Quantitation of PI(4,5)P_2 extraction from PM by PM-recruited ORP5/8. HEK293-AT1 cells were transfected and subjected to BRET measurement as described in A except that PM PI(4,5)P_2 levels were quantitated by measuring emission intensity of PM-anchored Venus from PLCδ1-PH–fused luciferase. Grand means ± SEM are shown from three independent experiments performed in triplicate. **(D)** Quantitation of cholesterol extraction from PM by PM-recruited ORP5/8. HEK293-AT1 cells were transfected with mCherry-FK-ORP5 and -ORP8 in addition to PM-anchoring FRB (PM2-FRB). PM cholesterol levels were quantitated by measuring emission intensity of PM-anchored Venus from D4H-fused luciferase. Treatment and measurements were performed as described in A. Grand means ± SEM are shown from three independent experiments performed in triplicate. **(E)** Extraction of cholesterol by treatment with methyl β-cyclodextrin (MβCD; 2 mM) was used to validate the method. Grand means ± SEM are shown from three independent experiments performed in triplicate.

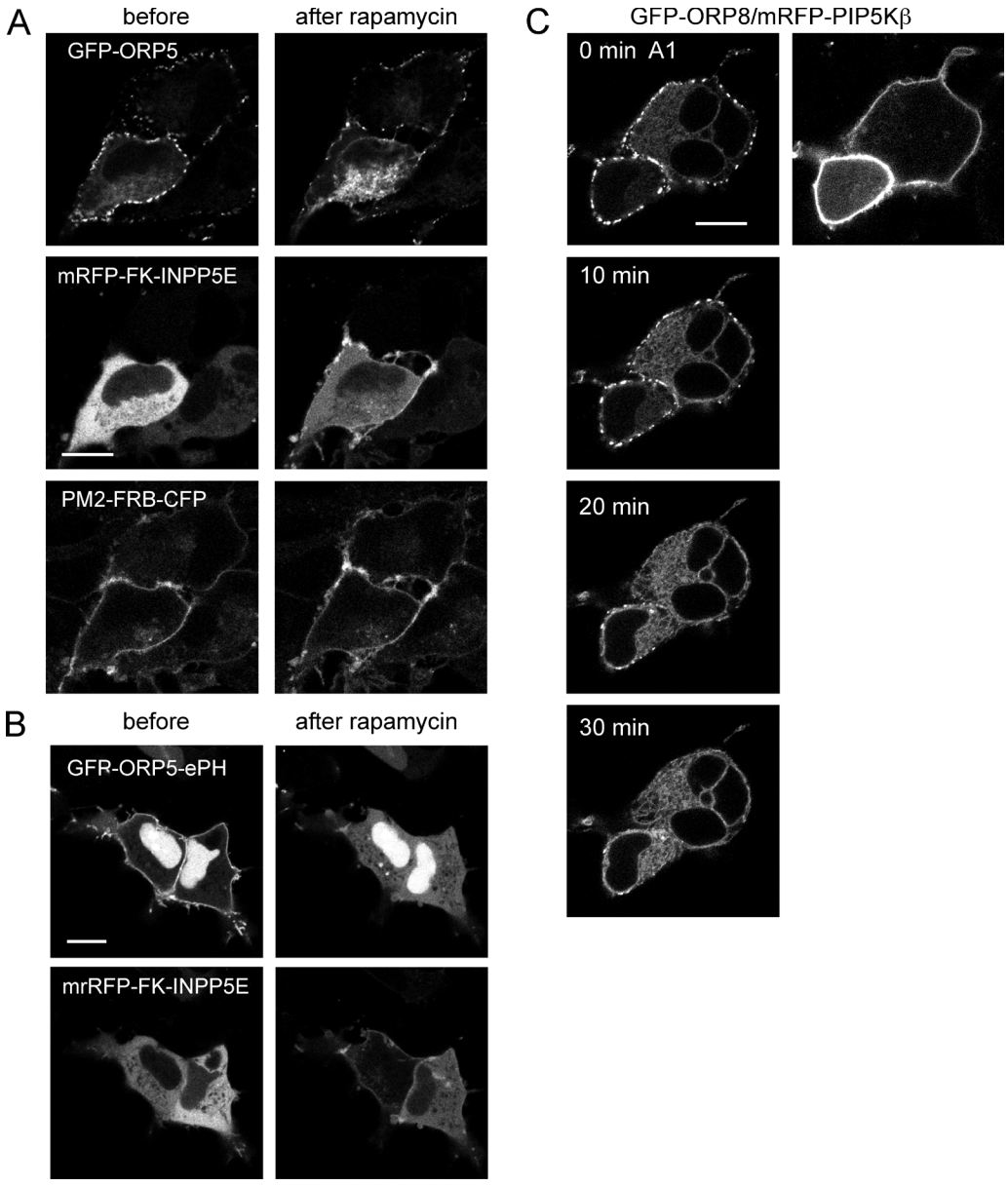

Figure S3. **Disengagement of ORP5 and ORP5-ePH from the PM in response to PM recruitment of INPP5E phosphatase. (A)** Representative live-cell image showing localization of ORP5 before and after recruitment of mRFP-tagged FKBP-INPP5E phosphatase to the PM. HEK293-AT1 cells were transfected with GFP-tagged ORP5, mRFP-tagged FKBP-INPP5E, and CFP-tagged PM2-FRB. After 1 d, cells were subjected to confocal microscopy before (left) and after (right) rapamycin treatment (100 nM, 5 min). **(B)** Representative live-cell image showing localization of ORP5-ePH before and after recruitment of mRFP-tagged FKBP-INPP5E phosphatase to the PM. HEK293-AT1 cells were cells GFP-tagged ORP5-ePH, mRFP-tagged FKBP-INPP5E, and CFP-tagged PM2-FRB. After 1 d, confocal microscopy was performed as described in A. **(C)** Cells were transfected with GFP-ORP8 and mRFP-PIP5Kβ to increase membrane interaction of ORP8. After 1 d of transfection, cells were treated with 100 nM A1, and the localization of GFP-ORP8 was followed by confocal microscopy. Note the slow dissociation of GFP-ORP8 from the PM and appearance in the ER. Bars, 10 µm.

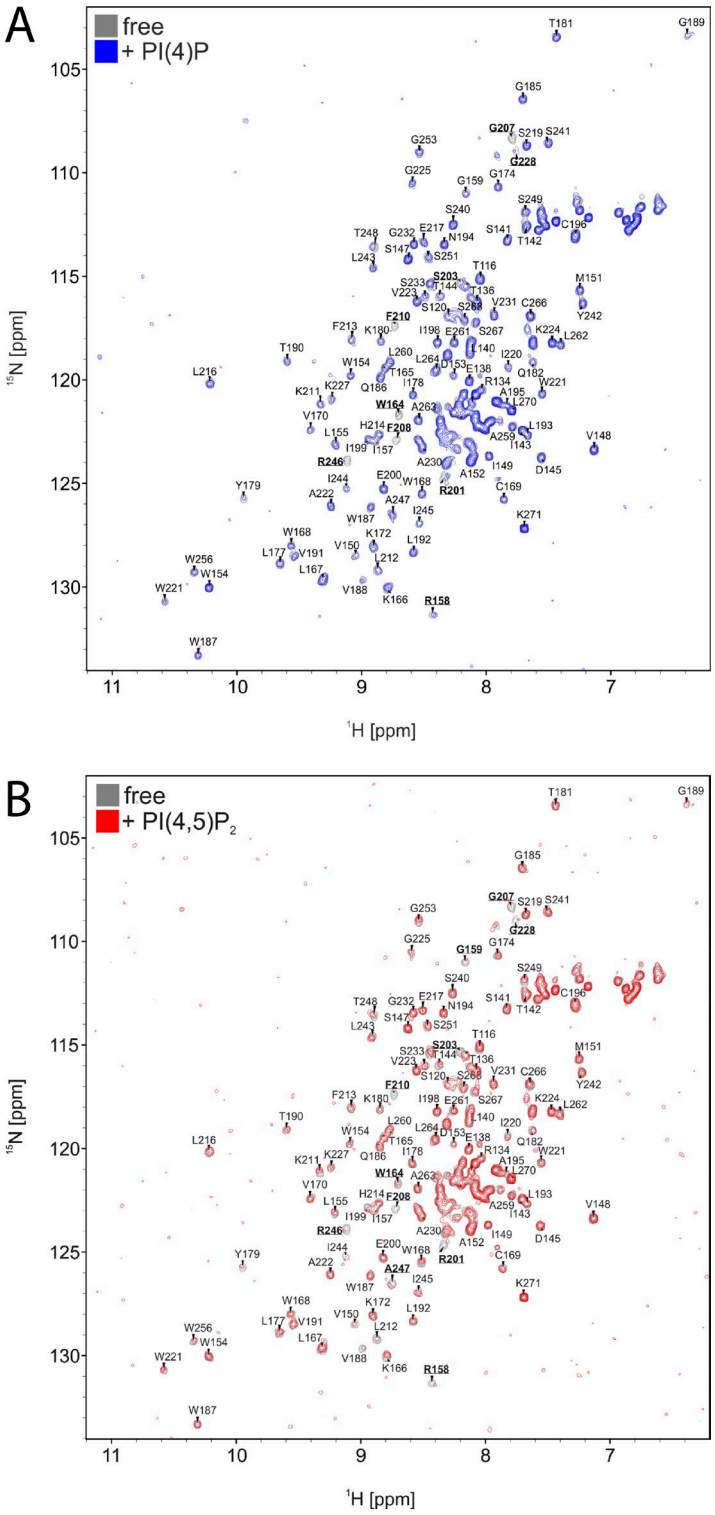

Figure S4. **PI4P and PI(4,5)P_2 binding to the ORP8 PH domain. (A)** Interaction of PI4P-induced specific changes in the 2D $^{15}N/^{1}H$ HSQC NMR spectra of ORP8. The labels of the most affected backbone amide signals of ORP8 are underlined. **(B)** Interaction of PI(4,5)P_2-induced specific changes in the 2D $^{15}N/^{1}H$ HSQC NMR spectra of ORP8. The labels of the most affected backbone amide signals of ORP8 are underlined. This figure includes directly observed NMR spectra for the free and ligand-bound protein in a single experiment.

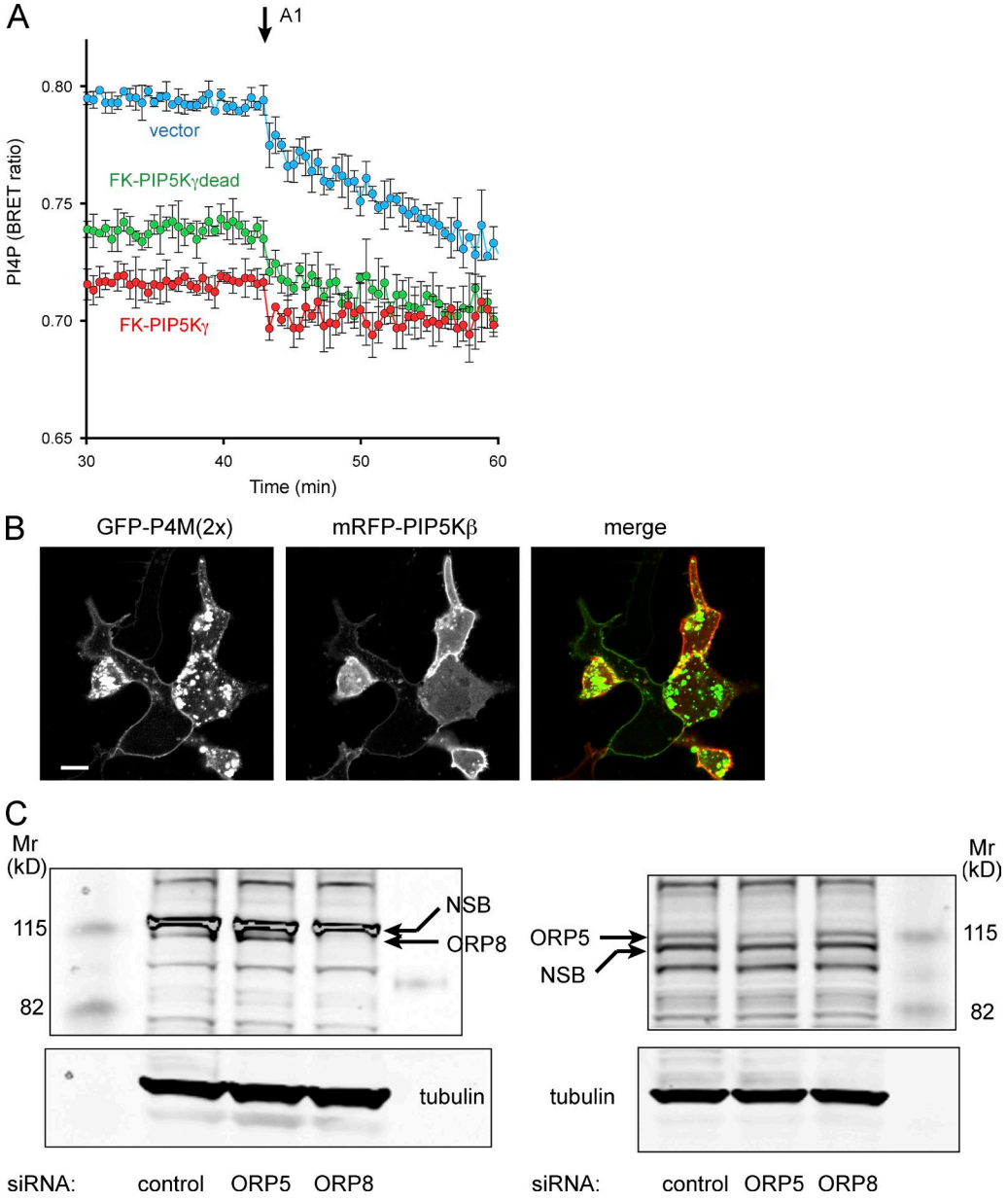

Figure S5. **Effects of PIP5K on PM PI4P levels. (A)** Representative BRET analysis monitoring PI4P clearance from the PM with or without PM-recruited PIP5Kγ. HEK293-AT1 cells were transected with CFP(W66A)-tagged FKBP-PIP5Kγ (wild-type or kinase-dead) and PM2-FRB 1 d before BRET measurement. Control cells were transfected with pcDNA3.1(HA) instead of FKBP-PIP5Kγ. PI4P clearance from the PM was analyzed with BRET by measuring emission intensity of PM-anchored Venus per P4M2x-fused luciferase. After baseline measurement and measurement with rapamycin (100 nM), cells were treated with A1 (30 nM), and PI4P clearance was monitored. Means ± SD are shown from triplicate experiments. **(B)** Representative live-cell image displaying redistribution of PI4P probe by PI5PKβ overexpression. HEK293-AT1 cells were transfected with GFP-tagged P4M2x and mRFP-tagged PIP5Kβ. After 1 d, cells were observed with confocal microscopy. Bar, 10 µm. **(C)** Western blot analysis of cellular extracts after knockdown of ORP5 and ORP8 proteins. NSB, nonspecific bands.

Table S1. **Primers used in this study**

Construct	Template DNA	Primers	Sequence (5′ to 3′)
GFP-ORP8-PLCδ1-PH	pEGFP-C3-ORP8	Forward	ATATGAGCTCAAACGTACAATGATCAGAGAAGGAAAGGAAC
		Reverse	ATATGTCGACACTGAGCAGCTCCTTTGTGGCTC
	pEGFP-N1-PLCδ1-PH	Forward	ATATGTCGACGAGGATCTACAGGCGCTGCTGAAG
		Reverse	ATATGAGCTCGTCCTTGTTTTTGTCAGCTTTTCGC
mRFP-PIP5Kβ	myc-PIP5Kβ	Forward	TATACAAGATCTCGATCGTCTGCTGCTGAAAATGGAGAG
		Reverse	ATATAGGTACCTTATAAATAGACGTCAAGCACAGAAGCATT
mRFP-PIP5Kβ-dead	mRFP-PIP5Kβ	Forward	TTTGACCTATGCCCTGAAAGGCTC
		Reverse	CCTTTCAGGGCATAGGTCAAATGCATC
GFP-ORP5-ePH	pEGFP-C1-ORP5	Forward	TATAGAATTCTTGCAACGGGTCAGACAAGGAATGTGTGTC
		Reverse	TATAGGTACCTACAGTCTCAGTAGGCTAGAGCAGCGCAGG
GFP-ORP8-ePH	pEGFP-C3-ORP8	Forward	TATAGAATTCTAGTTCAACTTCAAGCAAACTCACAAAAAAAGAATCTC
		Reverse	TATAGGTACCTATTTAAGAAGACTAGAACATTTCAAAGCCAACTCCAAAGCATCC
GFP-ORP5-PH	pEGFP-C1-ORP5	Forward	TATAGAATTCTGCTCTGACAGACCCCAGCGTGGTCATC
		Reverse	TATAGGTACCTACAGTCTCAGTAGGCTAGAGCAGCGCAGG
GFP-ORP8-PH	pEGFP-C3-ORP8	Forward	TATAGAATTCTACAATCACAGATCCTTCTGTTATTGTTATGGCTGATTGG
		Reverse	TATAGGTACCTATTTAAGAAGACTAGAACATTTCAAAGCCAACTCCAAAGCATCC
GFP-ORP8 ΔN (1-109)	pEGFP-C3-ORP8	Forward	ATATTGTACAACAGTTCAACTTCAAGCAAACTCAC
		Reverse	ATATCCCGGGTTACTTGAACATGAAGTTTATTATGACTTGAAGC
Cherry-FKBP-ORP5	mRFP-FKBP12-INPP5E	Forward	ATGCAAGCTTACTGGGAGTGCAGGTGGAAACCATC
		Reverse	AATATGCGATCGCAGCTTCCAGTTTTAGAAGCTCCACATCG
	pEGFP-C1-ORP5	Forward	ATAGCGATCGCAACCTGCAAGCCGGGCCGAGAC
		Reverse	ATATAAGCTTGCGCTGAGCAGCTGCCGTGTGGC
mCherry-FKBP-ORP8	mRFP-FKBP12-INPP5E	Forward	ATATGTCGACCTGGGAGTGCAGGTGGAAACCATC
		Reverse	ATATGAGCTCAGCTTCCAGTTTTAGAAGCTCCACATCG
myc-PIP5Kβ-dead	myc-PIP5Kβ	Forward	TTTGACCTATGCCCTGAAAGGCTC
		Reverse	CCTTTCAGGGCATAGGTCAAATGCATC
CFP(W66A)-FKBP-PIP5Kγ, CFP(W66A)-FKBP-PIP5Kγ-dead	CFP-FKBP-PIP5Kγ	Forward	TGCGGTCAGGGTGGTCACGAGGGTG
		Reverse	GGCGTGCAGTGCTTCAGCCGCTAC